Progress In Electromagnetics Research, PIER 102, 249–265, 2010

UNIFIED DESIGN PROCEDURE FOR PLANAR DIPOLES ORIENTED ON UWB APPLICATION

M. Pergol and W. Zieniutycz

Gdansk University of Technology
11/12 Narutowicza Str. 80-233, Gdansk, Poland

Abstract—In the paper, the unified design procedure for planar dipoles oriented on UWB application is proposed. The procedure leads to obtain a good matching characteristic of planar dipoles in UWB frequency band. The design process is split into two parts: the radiator and the balun design. The Radiator Quality Factor (RQF) is defined as an evaluation suitability of planar radiators to be matched in UWB frequency band. Based on RQF, the optimal circular radiator is chosen, and the whole dipole antenna is designed. The general algorithm of antenna design is formulated and utilised in the planar dipole with elliptical arms project. Two antennas, with circular and elliptical arms, have been fabricated and measured in order to verify the design procedure. Both antennas are characterized by the reflection coefficient less than −10 dB from 2 GHz up to 14 GHz.

1. INTRODUCTION

UWB is still a developing and promising technology theoretically extending our abilities in fast transmission of imense amounts of data. Many devices oriented on this technology are currently investigated in order to fulfill the specific requirements [1]. Therefore, it is reasonable to expect that the antennas for UWB will be the object of R&D activity as well. There are many types of antennas that are suitable for UWB applications, e.g., horn antennas, Vivaldi antennas, monopoles and dipoles. Vivaldi antennas, thanks to their directivity and good dispersion characteristic can be applied to radar techniques. Monopoles and dipoles with nondirectional radiation pattern are better for communication systems [2].

Lately, we can find many publications concerning unbalanced plannar antennas as a smart and suitable ones for UWB applica-

Corresponding author: M. Pergol (mper@eti.pg.gda.pl).

tions [3, 4]. However, there are only few publications focused on balanced plannar antennas. The following two groups of papers can be distinguished among the works concerning applied analysis of this antenna type: (i) publications covering only separated radiators (e.g., [5–10]); (ii) publications focused on the antennas as a whole (e.g., [11–17]).

The first group of publications shows in most cases only numerical results with arbitrarily chosen reference impedance [5, 9, 10] or does not provide any information about it [6–8]. As an example of application of such results the authors indicate an ability of connection radiators with a differential amplifier [9, 10]. There are also some papers analysing separated radiators, for which both simulated and measured results are given, however in this cases, the radiators seemed to be connected directly to an unbalanced line [7, 8].

The second group of papers contains analysis of the entire balanced antennas (balun and radiators): antipodal ones, for which the whole antenna is optimised [14–16] and coplanar ones, for which a balun is designed first and then the antenna is optimised [11–13]. In most of these publications the characteristic impedance of coplanar lines (CPS) is arbitrarily chosen without any explanation on the criteria of such a choice.

The last group of papers focuses on dipoles fed by unbalanced lines (CPW), however, these dipoles are in fact monopoles with modified ground plane [17].

This short review shows some problems which this work faces: the radiator analysis seldom exists and the criterion of choice of reference impedance is not investigated. Due to this fact: (i) the choice of radiator shape is generally not optimal; (ii) the dimensions of CPS in baluns' balanced port and in the input port of radiator are chosen arbitrarily (and generally in not an optimal way as well).

Based on aformentioned issues this work introduces unified design procedure of planar balanced antennas for UWB application. Special attention is focused on the optimal choice of radiator's shape and feeding CPS lines. In this work the radiator quality factor, introduced in [19], is further developed. In [19], the reference impedance was chosen independently of the feeding line structure. In this contribution, the reference impedance is directly related to the characteristic impedance of the feeding line, so the optimisation of feeding line is also available. According to the proposed procedure the whole antenna is split into smaller parts (radiator, feeding lines, balun) in order to design and optimise them separately. This procedure leads to easier and faster design of an antenna.

In Section 2, we define the radiator quality factor (RQF) as

a consequence of the proper choice of reference impedance. This factor is then applied in order to choose the optimal structure (in terms of minimal reflection coefficient) of exemplary circular dipole arms. After having established the optimal circular dipole structure, a suitable balun is designed and the reflection coefficient of the whole antenna is calculated in Section 2.2.3. As an example of application of unified design procedure, the dipole with elliptical arms is designed in Section 3. The final part of the paper presents the conclusions.

2. METHOD OF DESIGNING

2.1. Radiator Quality Factor (RQF)

In general case, any planar dipole antenna consists of two parts: radiator with its feeding strips (CPS) and balun. A radiator is characterized by input impedance $Z_r(f)$, which connected to an ideal, non-dispersive line determines the reflection coefficient of radiator:

$$\Gamma_{rad}(f) = \frac{Z_r(f) - Z_0^{ref}}{Z_r(f) + Z_0^{ref}} \tag{1}$$

where Z_0^{ref} is a characteristic impedance of the connected line, treated here as a reference impedance. Z_0^{ref} can be chosen arbitrary, however, it has been shown in [19], that for any radiator operating in defined frequency band there exists an optimal reference impedance Z_0^{opt} for which the maximal value of $|\Gamma_{rad}(f)|$:

$$\Gamma_{opt}(f) = \frac{Z_r(f) - Z_0^{opt}}{Z_r(f) + Z_0^{opt}} \tag{2}$$

is minimal. We have verified that the reference impedance has small reactive part, so the reference resistance can be treated as the characteristic impedance of feeding line.

After these preliminary remarks we consider more realistic model where a planar radiator is connected by a CPS line to the balun characterized by scattering matrix $S_{2\times 2}$ (Fig. 1). We observe that the significant part of the feeding line should be treated as an element of the radiator (Fig. 2). We denote the characteristic impedance of this line, when calculated in the absence of radiating arm, as $Z_0^{int}(f)$ (see Fig. 2). In this case, the reference impedance is equal to the characteristic impedance of the radiator feeding line, so $\Gamma_L(f)$ is expressed as follows:

$$\Gamma_L(f) = \frac{Z_r(f) - Z_0^{int}(f)}{Z_r(f) + Z_0^{int}(f)}. \tag{3}$$

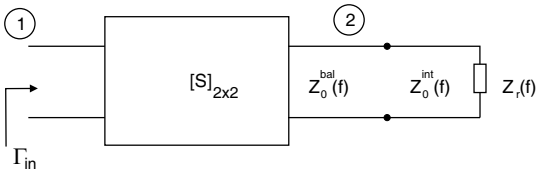

Figure 1. Scheme of the antenna-radiator connected to a balun defined by the scattering matrix.

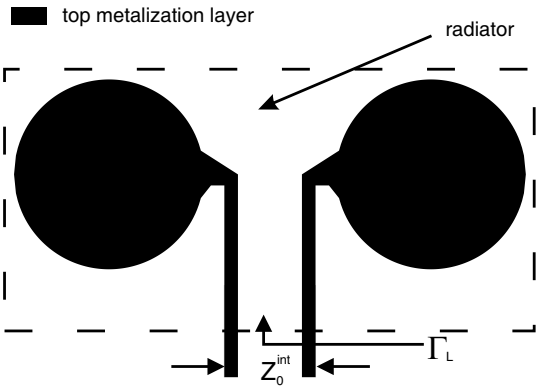

Figure 2. Scheme of the radiator arms with its feeding lines.

It is obvious from Eqs. (3) and (2) that our design procedure should assure the following optimal choice:

$$Z_0^{int}(f) = Z_0^{opt} \tag{4}$$

We have verified using ADS Momentum, that the frequency dispersion of the impedance $Z_0^{bal}(f)$ is small enough (about 7% in the whole UWB band), so we modify condition (4) to the following form:

$$Z_0^{int}(f = f_0) = Z_0^{opt} \tag{5}$$

where f_0 is the middle frequency of UWB ($f_0 = 6.85\,\mathrm{GHz}$). In order to avoid the discontinuity between the impedances Z_0^{int} and Z_0^{bal} we enforce the condition (5) to the form:

$$Z_0^{bal}(f = f_0) = Z_0^{int}(f = f_0) = Z_0^{opt} \tag{6}$$

We should underline that every radiator is characterised by its own optimal impedance Z_0^{opt}. Therefore, an arbitrary choice of the impedance $Z_0^{bal}(f)$ (and corresponding CPS configuration at the output port of the balun) should not generally lead to an optimal shape

of radiator. It is because in most cases arbitrarily chosen impedance $Z_0^{bal}(f)$ is not equal to Z_0^{opt}. Thus Eq. (6) forms the basic design condition which offers the optimal choice of the radiator shape from the point of view of broadband matching.

In order to introduce a radiator quality factor (RQF) we assume, that the radiator is connected to the optimal feeding line with characteristic impedance fulfilling condition (6). The maximal value of $|\Gamma_{opt}(f)|$ within the entire analysed frequency band is denoted as $\Gamma_{\max}$. We propose to define RQF as a maximal value of SWR over the whole analysed frequency band:

$$RQF = SWR_{\max} = \frac{1 + \Gamma_{\max}}{1 - \Gamma_{\max}}. \tag{7}$$

The less the RQF is, the better the radiator (in terms of the broadband impedance matching) is. We underline that RQF corresponds to the optimal choice of the feeding line impedance on the output port of balun. Such choice of the impedances (according to the condition (6)) is unique, so RQF can be treated as a measure of the quality of the radiator.

2.2. Algorithm of the Antenna Design

In order to illustrate an application of RQF in the radiator design we consider circular radiator, which is fed by a CPS line from balun. The whole issue is separated into two problems: the radiator design and the balun design. Thanks to this operation the optimal radiator can be found and then, the corresponding balun can be optimised.

2.2.1. Radiator Design Description

The circular radiator is shown in Fig. 3. The reason of choice of the circular radiator is a small number of parameters to optimize.

The radiator consists of two symmetrical parts described in Table 1. Each of the parts consists of three elements which are characterized by one parameter:

- the proper radiator, characterized by the radius of the circle r,
- the coupling element, characterized by its height c,
- the feeding lines, characterized by the distance between them s.

Each of these elements influences the input impedance of the radiator in a very significant way. The remaining parameters of the radiator are fixed.

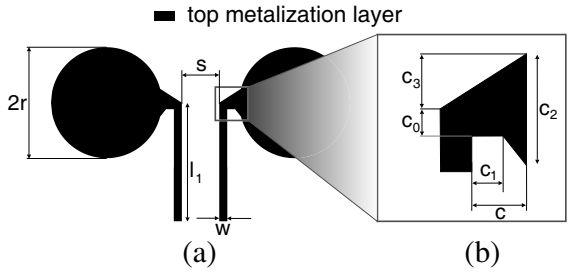

Figure 3. Circular radiator: (a) general view, (b) the coupling structure between circular arm and feeding line.

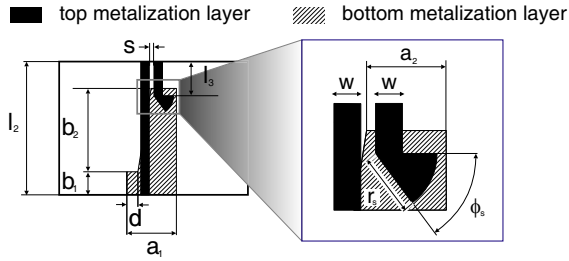

Figure 4. Balun scheme.

Table 1. Definitions and parameters of the circular radiator.

c_0 [mm]	c_1	c_2 [mm]	c_3 [mm]
1.4	$(2/3) \cdot c$	5.4	3

This radiator is to be connected to balun (Fig. 4), which adjusts the input impedance of the radiator to the 50 Ω standard in general case [18].

The transformation of the electromagnetic field between microstrip line and coplanar striplines is made due to the tapered ground plane and application of the radial stub. The only fixed parameters of the balun are: (i) the width of the microstrip line (it should make the microstrip line characterized by 50 Ω impedance) and (ii) the width of the CPS lines. Both parameters (denoted as w) are equal to each other, so that the geometrical discontinuities between microstrip and CPS line do not occur. The distance s is restricted to be the same as the distance between feeding lines in radiator due to the aforementioned reason.

In the first step of any antenna design, the substrate should be

chosen, on which the antenna will be made. Let us take a substrate of $\epsilon_r = 3.5$ and $h = 0.76\,\text{mm}$ (Taconic RF35). The first parameter which should be fixed is a width $w = 1.72\,\text{mm}$ of the microstrip line. It assures the characteristic impedance of the microstrip line to be $50\,\Omega$. Other dimensions defining the coupling element structure are presented in the Table 1.

After the parameter w is set, our attention is focused on the parameters: s, c and r, which is to be optimized. We propose an iterative procedure, so the first approximations is denoted as $s^{(1)}$, $c^{(1)}$ and $r^{(1)}$. All simulations are performed in ADS Momentum environment.

We start with the choice of the parameter $s^{(1)}$ which influences the characteristic impedance of CPS and should fulfill the condition (6). Although the optimal impedance Z_0^{opt} is unknown, the knowledge of its range is well known. Theoretically, infinitely broadband antennas are characterized by invariant input impedance equal to $60\pi\,\Omega$ [20]. However, in real planar antennas input impedance depends on shape and size of the radiator and it changes approximately from $110\,\Omega$ up to $180\,\Omega$. As a consequence, the Z_0^{opt} and the characetristic impedance of CPS should be within this range. Let us take $Z_0^{int}(f_0) = 151\,\Omega$. We can calculate the corresponding parameter $s^{(1)}$ equal to 0.95 mm. Now, we find the first approximations $c^{(1)}$ and $r^{(1)}$.

The parameter c determines the distance between radiator arms. It is especially important in the case of circular arms which can not start on the feeding lines ($c = 0\,\text{mm}$). On the other hand, in order to minimize the radiator size, the distance should be as small as possible. We propose to take $c^{(1)} = 0.4\,\text{mm}$.

After the first two parameters ($s^{(1)}$, $c^{(1)}$) have been fixed, we start by examining the radius influence on RQF. The results of calculations of RQF and Z_0^{opt} as a function of r are shown in Fig. 5.

The RQF curve is characterized by the minimum equal to 1.45 which occurs at $r = 12\,\text{mm}$. The optimal impedance Z_0^{opt} for this point is equal to $152.7\,\Omega$ which is almost equal to the characteristic impedance of the line $Z_0^{int}(f_0) = 151\,\Omega$. Thus, the $r^{(1)} = 12\,\text{mm}$ is the optimal value and the first loop of the iterative design procedure for variable r is closed. Now, we examine the loop of the variable c in order to find its second approximation $c^{(2)}$. The results of such an opertion are shown in Fig. 6.

The character of the curve in Fig. 6 is similar to the curve in Fig. 5. A minimum of RQF can be observed at $c = 1.0\,\text{mm}$ and the optimal impedance at this point $Z_0^{opt} = 143\,\Omega$ is still close to the impedance $Z_0^{int}(f_0)$.

As a result, we can establish $c^{(2)} = 1\,\text{mm}$ as a second approximation of c and the first loop of the iterative design procedure for variable c is closed. The obtained result finalizes the important step of the procedure of finding the best radiator. Now we can repeat the procedure for different values of s (the most external loop) until the optimal dimensions of radiator are found. Such calculations were made and they showed that the radiator charcterized by the following parameters: $c = 1.0\,\text{mm}$, $r = 12\,\text{mm}$, $s = 0.95\,\text{mm}$ (corresponding $Z_0^{int}(f_0) = 151\,\Omega$) offers the best value of RQF equal to 1.33. This radiator is treated as the optimal one and it is examined in further stages of design. In Fig. 7, the exemplary results of the curves $RQF = f(c)$ are presented for different combinations of s and r.

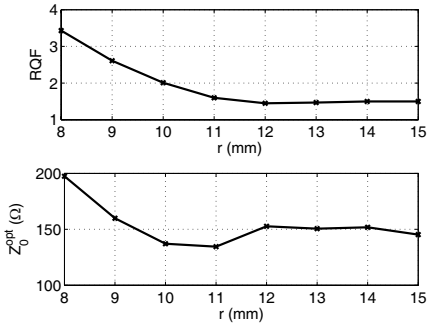

Figure 5. RQF and Z_0^{opt} as a function of radius r; calculation for $s^{(1)} = 0.95\,\text{mm}$; $c^{(1)} = 0.4\,\text{mm}$.

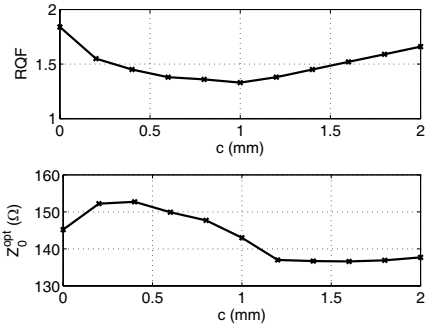

Figure 6. RQF and Z_0^{opt} as a function of c; the remaining parameters: $s^{(1)} = 0.95\,\text{mm}$; $r^{(1)} = 12\,\text{mm}$.

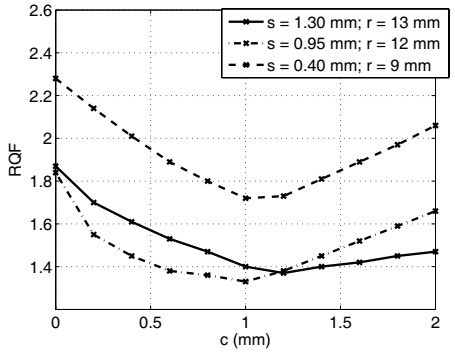

Figure 7. Family of characteristics for different s and r.

We can observe the distinct minima for every curves, which seems to prove that iterative procedure can be applied in design process of such radiators.

2.2.2. Flow Graph of the Radiator Design Procedure

In the previous section the method of finding the optimal radiator has been described. In fact, two main stages can be there distinguished:

- Choice of substrate and some parameters which remain fixed during the optimization (e.g., width of the strip w, that determines the impedance of input port of antenna to be $50\,\Omega$). Some parameters belonging to this group are chosen arbitrary (e.g., dimensions of coupling structure). These parameters form the data vector of length M which will be denoted as **inv**.
- Determination of the radiator parameters s, c, r which yields the minimal value of RQF. During the optimization procedure we are looking for optimal values of the variables which form the data vector of length N, denoted as **var**.

  Thus, RQF is a function of these two vectors:

$$RQF = f(\mathbf{inv}, \mathbf{var}) \tag{8}$$

and the algorithm should minimize (8) for given **inv**.

The proposed iterative design procedure can be presented in a flow graph form (Fig. 8). The algorithm starts with choice of vector **inv**. Next, the vector **var** is defined, as well as the ranges of the changes of its elements. The RQF is then calculated for different values of **var** until the RQF minimum is achieved. At the same time the differences between optimal impedances Z_0^{opt} and characteristic impedances Z_0^{int} are checked. If these differencies are sufficiently small (less than $\Delta_{\max}$), the algorithm comes to a conclusion and we decide whether the results are acceptable.

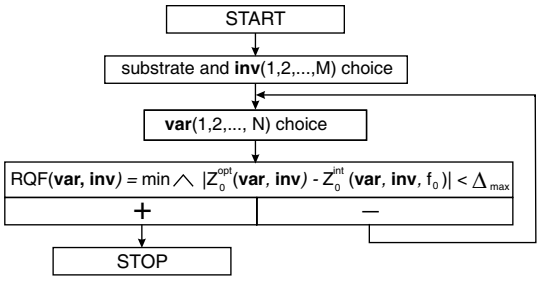

Figure 8. Flow graph of designing radiator procedure.

2.2.3. Balun Design and Simulation of the Whole Antenna

As a result of proposed algorithm, the optimal radiator has been selected. In order to obtain a project of whole antenna, the proper balun should be designed. As an example let us take selected before optimal circular radiator, characterized by the following data vectors:

$$\mathbf{inv} = [w\ l_1\ a_1\ b_1] = [1.72\ 28\ 10\ 2] \tag{9}$$

$$\mathbf{var} = [s\ c\ r] = [0.95\ 1\ 12] \tag{10}$$

and the balun type shown in Fig. 4.

The remaining parameters, namely, $l_2, l_3, a_2, b_2, d, \phi_s, r_s$ are to be optimized. The balun is loaded by the input impedance of the circular radiator (see Fig. 9) as it is shown in Fig. 1, so that the reflection coefficient of the whole antenna Γ_{in} can be calculated. Thanks to the fact, that the balun is only simulated, not the whole antenna, the immense time saving is obtained. The input impedance of the radiator shown in Fig. 9 changes from $113\,\Omega$ up to $190\,\Omega$ in its real part and from $-35\,\Omega$ up to $34\,\Omega$ in its immaginary part. What is important to see, the imaginary part is much less than the real part and it is focused close to zero. It confirms our assumption that the radiator can be matched to the line of which characteristic impedance is found as Z_0^{opt}.

Due to the dispersion occured in CPS, the reflection coefficient Γ_L is calculated and compared with optimal one Γ_{opt} in Fig. 10. The chart confirms validity of definition and application of $|\Gamma_{opt}|$, whose level is only a bit greater than level of $|\Gamma_L|$.

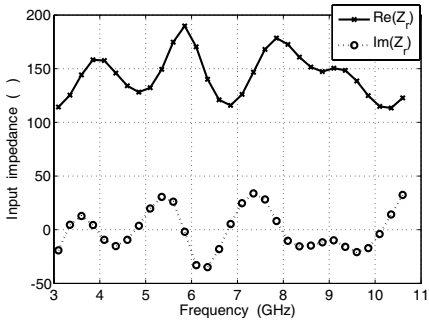

Figure 9. Input impedance of the circular radiator with geometrical parameters given in (9), (10).

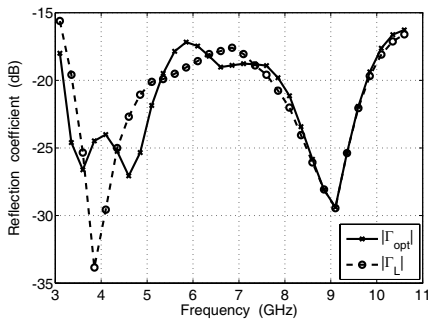

Figure 10. Reflection coefficient of the circular radiator: with dispersion of CPS (solid line), without dispersion (dotted line).

After the optimal parameters of the balun have been found, the final balun is loaded by the real radiator, and the whole antenna is simulated for final tuning. The small differences between optimising results (when balun loaded by radiator impedance Z_r) and results of the whole antenna simulation are compensated by changing the length of the feeding lines (l_1). The numerical results of final simulation of whole antenna reflection are shown in Fig. 11. The antenna is characterized by small reflection coefficient in the whole UWB band. The maximum occurs at 7.9 GHz and is equal to -14.41 dB (SWR $= 1.47$). The final dimensions of the antenna are shown in Table 2.

The antenna has been designed using the algorithm proposed in this paper. The same results could be achieved by optimisation of a whole antenna, only if the starting point were properly chosen. However, in this case, the knowledge of radiator quality, which can be used in other antenna structures (e.g., the optimal radiator can be connected to another balun or to differential amplifier), is lost. Also, the simulation time of balun loaded by the radiator impedance is about 75% shorter than the time of whole antenna simulation.

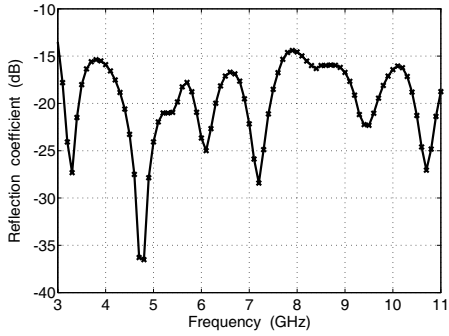

Figure 11. Reflection coefficient simulated for the whole antenna with circular arms.

Table 2. The final parameters of the antenna. All dimensions in [mm] (apart from ϕ_s [deg]).

c_0	1.40	r	12.00	a_1	10.00
c_1	0.66	c	1.00	a_2	4.72
c_2	5.40	l_1	30.00	b_1	2.00
c_3	3.00	l_2	10.00	b_2	18.24
w	1.72	l_3	20.00	r_s	3.94
s	0.95	d	2.23	ϕ_s	53.38

3. CASE STUDY — ELLIPTICAL RADIATOR DESIGN

In the previous section, the algorithm of the optimal radiator search, resulting in the whole antenna design, has been proposed. Now, the presented procedure is implemented in the case of elliptical radiator type. Following the concept shown in Fig. 8, we start with a substrate and a type of balun choice. In order to define a vector **inv** let us take the same substrate ($\epsilon_r = 3.5, h = 0.76\,\text{mm}$) and the same balun type as in the circular radiator case. Thanks to this, comparison of two antennas (with circular and elliptical arms) is possible. The scheme of the balun type and the elliptical radiator are shown in Figs. 4 and 12, respectively.

As a consequence of such a choice, the vector **inv** can be expressed in the following form:

$$\mathbf{inv} = [w\ l_1\ c_1\ c_2\ c_3] = [1.72\ 28\ 1.4\ 5.4\ 3] \tag{11}$$

In turn, the vector **var** defined as follows:

$$\mathbf{var} = [s\ c\ r_1\ r_2] \tag{12}$$

has been optimised, based on the concept presented in Fig. 8. The start point of vector **var** has been defined as:

$$\mathbf{var}^{(1)} = [s^{(1)}\ c^{(1)}\ r_1^{(1)}\ r_2^{(1)}] = [0.7\ 1.0\ 12\ 8] \tag{13}$$

and after 3 iterations of s, 2 iterations of c, 2 iterations of r_1 and 1 iterations of r_2, the minimal value of RQF has been achieved:

$$RQF = f(\mathbf{inv}, \mathbf{var}) = f([1.72\ 28\ 1.4\ 5.4\ 3], [0.9\ 1.0\ 12\ 11]) = 1.30 \tag{14}$$

Total number of the iterations for this case is equal to $3 \cdot 2 \cdot 2 \cdot 1 = 12$. This number depends on the proper choice of starting point, so the designer experience is an important factor in the design efficiency. The value of $s = 0.9\,\text{mm}$ determines the characteristic impedance of

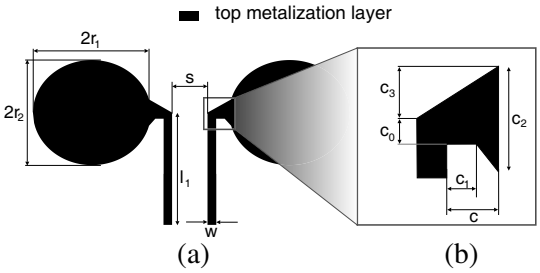

Figure 12. Elliptical radiator: (a) general view; (b) the coupling structure between the circular arm and the feeding line.

the feeding line $Z_0^{int}(f_0)$ to be equal to $148\,\Omega$. In turn, the optimal impedance Z_0^{opt} selected for **inv**, **var** defined in the Eq. (14) equals $143\,\Omega$. Such a small difference confirms that this elliptical radiator is well-matched to the feeding line.

The input impedance of the optimal elliptical radiator is shown in Fig. 13. The curves of the input impedance of elliptical radiator are similar to those of circular radiator. It is expectable because both radiators are similar. However, different characteristic impedance of the feeding line $Z_0^{int}(f_0)$ and smaller amplitude of the input resistance of the elliptical radiator results in smaller value of RQF. In turn, the level of reflection coefficient of the whole antenna $|\Gamma_{in}|$, calculated after the proper balun design, is the same as in the case of circular radiator (see Fig. 14).

The final dimensions of the antenna with elliptical arms after final tuning are shown in the Table 3.

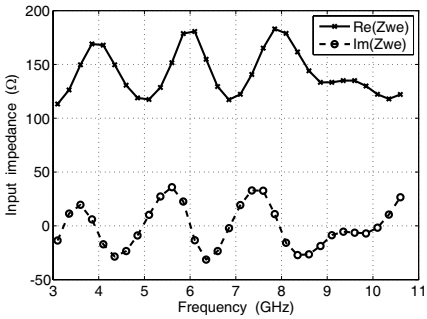

Figure 13. Input impedance of the elliptical radiator.

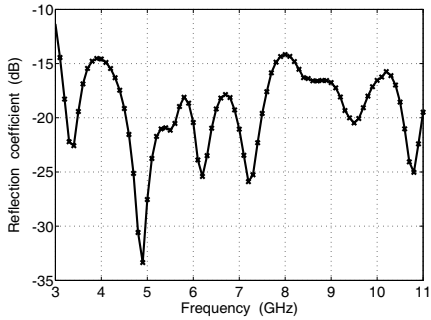

Figure 14. Simulated reflection coefficient of the whole antenna with elliptical arms.

Table 3. The final parameters of the antenna with elliptical arms. All dimensions in [mm] (apart from ϕ_s [deg]).

c_0	1.40	r_1/r_2	12.00/11.00	a_1	10.00
c_1	0.66	c	1.00	a_2	4.77
c_2	5.40	l_1	29.00	b_1	2.00
c_3	3.00	l_2	10.00	b_2	18.09
w	1.72	l_3	20.00	r_s	3.68
s	0.90	d	2.14	ϕ_s	62.39

Note, that the final parameters of the antenna are the local minimum of the function (Eq. (8)). The global minimum could be found by using other optimization method, e.g., genetic algorithm.

4. MEASUREMENTS

The numerical results of the antennas with circular and elliptical arms have been presented in Sections 2 and 3. Then, the antennas have been fabricated (see Figs. 15, 16) and the reflection coefficient has been measured. The comparison of the numerical and experimental results are shown in Figs. 17, 18. We can observe a good agreement in terms of character of both, experimental and numerical curves. The differences between them, occurred especially in the upper frequency region, can be caused by the SMA connector, whose presence was neglected in the simulations. Both antennas are characterized by the reflection coefficient less than $-14\,\mathrm{dB}$ (SWR < 1.5) in almost entire UWB frequency band. Only at a small frequency range (from about $8\,\mathrm{GHz}$ up to $9.5\,\mathrm{GHz}$) the reflection coefficient is a bit greater. The reflection coefficient less than $-10\,\mathrm{dB}$ occurs from $2.8\,\mathrm{GHz}$ up to at least $14\,\mathrm{GHz}$ for both antennas.

Additionally, the radiation patterns have been measured. The results do not diverge from ones presented in publications concerning printed dipole antenna with elliptical arms (e.g., [21, 22]). The antenna is characterized by omni-directional radiation pattern in H-plane at lower frequencies. At higher frequencies some disturbances occure, because of the SMA connector presence.

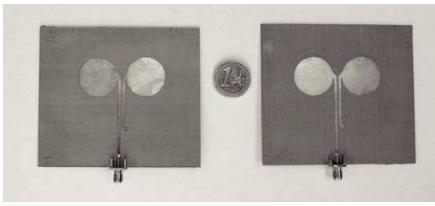

(a) (b)

Figure 15. The top of the antennas; (a) circular one; (b) elliptical one.

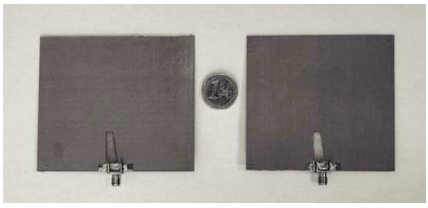

(a) (b)

Figure 16. The bottom of the antennas; (a) circular one; (b) elliptical one.

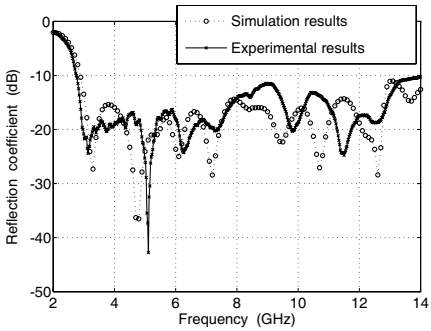

Figure 17. Comparison of the reflection coefficient for the antenna with circular arms.

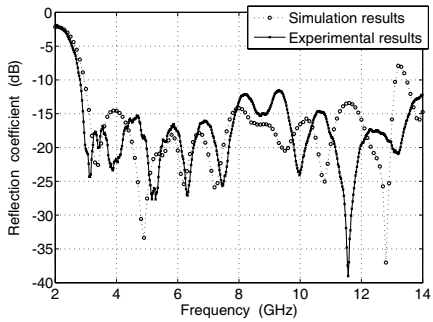

Figure 18. Comparison of the reflection coefficient for the antenna with elliptical arms.

5. CONCLUSION

In the paper, the unified design procedure for planar dipole oriented on UWB application has been presented. The algorithm has been formulated on the basis of circular radiator case study. Using the proposed algorithm, two optimal planar radiators (in terms of the minimal reflection coefficient) have been selected and two whole antenna structures have been designed. Then, the antennas have been fabricated and experimentally verified with numerical results in order to check the proposed procedure. The experimental results are satisfactory and a good agreement between numerical and experimental results has been achieved, especially at lower frequencies. The measured antennas are characterized by very small reflection coefficient in the whole UWB frequency band. Presented results confirm that the algorithm can be efficiency applied to design of planar dipoles oriented on UWB application.

ACKNOWLEDGMENT

This work is partially supported from the sources for science under the ordered scientific project PBZ-MNiSW-02/II/2007.

REFERENCES

1. FCC, "First report and order," *Revision of Part 15 of the Commissions Rules Regarding Ultra Wideband Transmission Systems*, ET Docket 98-153, FCC 02-48, 2002.

2. Wiesbeck, W., G. Adamiuk, and C. Sturm, "Basic properties and design principles of UWB antennas," *Proceedings of the IEEE*, Vol. 97, No. 2, 372–385, 2009.
3. Lin, C.-C. and H.-R. Chuang, "A 3–12 GHz UWB planar triangular monopole antenna with ridged ground-plane," *Progress In Electromagnetics Research*, PIER 83, 307–321, 2008.
4. Zaker, R., C. Ghobadi, and J. Nourinia, "A modified microstrip-FED two-step tapered monopole antenna for UWB and WLAN applications," *Progress In Electromagnetics Research*, PIER 77, 137–148, 2007.
5. Cerny, P. and M. Mazanek, "Optimized ultra wideband dipole antenna," *18th Int. Conf. on Applied Electromagnetics and Communications*, 1–4, 2005.
6. Duncan, C. and E. Lule, "Half disc element dipole antenna," *IEEE Antennas and Propagation Society Int. Symposium*, Vol. 4A, 189–192, 2005.
7. Lule, E., T. Babi, and K. Siwiak, "Diamond dipole antenna for ultra-wideband communications," *Microwave and Optical Technology Lett.*, Vol. 46, No. 6, 536–538, 2005.
8. Horita, A. and H. Iwasaki, "A planar dipole antenna with wideband characteristics for UWB and wireless LAN," *Electronics and Communications in Japan*, Vol. 90, No. 12, 22–30, 2007.
9. Quintero, G. and A. K. Skrivervik, "Analysis of planar UWB elliptical dipoles fed by a coplanar stripline," *IEEE Int. Conf. on Ultra-wideband*, Vol. 1, 113–116, 2008.
10. Chan, K. C. L. and Y. Huang, "A novel CPS-fed balanced wideband dipole for ultra-wideband applications," *First European Conf. on Antennas and Propagation*, 1–4, 2006.
11. Kim, Y.-G., D.-S. Woo, K. W. Kim, and Y.-K. Cho, "Design of bow-tie-type UWB antennas using an ultra-wideband balun," *IEEE Antennas and Propagation Society Int. Symposium*, 1989–1992, 2007.
12. Vahdani, M. and X. Begaud, "Wideband integrated CPS-fed dual polarized quasi bow-tie antenna," *Microwave and Optical Technology Lett.*, Vol. 51, No. 9, 2130–2136, 2009.
13. Guo, Y. X., Z. Y. Zhang, L. C. Ong, and M. Y. W. Chia, "A new balanced UWB planar antenna," *Microwave and Optical Technology Lett.*, Vol. 49, No. 1, 114–118, 2006.
14. Gao, G.-P., X.-X. Yang, J.-S. Zhang, J.-X. Xiao, and F.-J. Wang, "Double-printed rectangular patch dipole antenna for UWB applications," *Microwave and Optical Technology Lett.*, Vol. 50,

No. 9, 2450–2452, 2008.

15. Dadgarpour, A., G. Dadashzadeh, M. Naser-Moghadasi, and F. Jolani, "Design and optimization of compact balanced antipodal staircase bow-tie antenna," *IEEE Antennas and Wireless Propagation Lett.*, Vol. 8, 1135–1138, 2009.
16. Carro, P. L. and J. de Mingo, "Ultrawideband parallel strip antennas designed by genetic algorithms," *IEEE 66th Vehicular Technology Conf.*, 2047–2050, 2007.
17. Su, S.-W. and K.-L. Wong, "Printed band-notched ultra-wideband quasi-dipole antenna," *Microwave and Optical Technology Lett.*, Vol. 48, No. 3, 418–420, 2006.
18. Tu, W.-H. and K. Chang, "Wide-band microstrip-to-coplanar stripline/slotline transitions," *IEEE Trans. Microwave Theory and Techniques*, Vol. 54, No. 3, 1084–1089, 2006.
19. Pergol, M. and W. Zieniutycz, "New planar dipole radiator for UWB application," *Int. Conf. on Microwaves, Radar and Wireless Communications, MIKON2008*, 1–4, 2008.
20. Balanis, C. A., *Antenna Theory Analysis and Design*, John Wiley & Sons, New York, 1982.
21. Pergol, M. and W. Zieniutycz, "UWB planar antenna dipole in the sandwich configuration," *Int. Conf. on Antenna Theory and Techniques ICATT'09*, 187–189, 2009.
22. Schantz, H. G., "Planar elliptical element ultra-wideband dipole antennas," *IEEE Symposium Antennas and Propagation Society International*, Vol. 3, 43–46, 2002.